Applied Thermal Engineering 124 (2017) 1112–1122

Contents lists available at ScienceDirect

Applied Thermal Engineering

journal homepage: www.elsevier.com/locate/apthermeng

Research Paper

Computational study of acoustic streaming and heating during acoustic hemostasis

Maxim A. Solovchuk [a,d,*], Marc Thiriet [b], Tony W.H. Sheu [c,d,*]

[a] National Health Research Institutes, Institute of Biomedical Engineering and Nanomedicine, Taiwan
[b] Sorbonne Universities, UPMC Univ Paris 06, UMR 7598, Laboratoire Jacques-Louis Lions, F-75005 Paris, France
[c] Center of Advanced Study in Theoretical Sciences (CASTS), National Taiwan University, Taiwan
[d] Department of Engineering Science and Ocean Engineering, National Taiwan University, No. 1, Section 4, Roosevelt Road, Taipei 10617, Taiwan

HIGHLIGHTS

- 3D three-field coupling physical model for investigation of acoustic hemostasis is presented.
- Acoustic streaming(AS) effect can reduce or completely stop the flow out of the wound.
- AS effect is studied for two wound shapes and different sonication angles.
- The study shows the theoretical possibility of sealing the bleeding site by focused ultrasound.
- Sonication angles between 450 and 900 should be considered in order to reduce blood flow out of the wound.

ARTICLE INFO

Article history:
Received 4 July 2016
Revised 5 May 2017
Accepted 8 June 2017
Available online 15 June 2017

Keywords:
Acoustic hemostasis
HIFU
Navier-Stokes equations
Acoustic streaming
Westervelt equation

ABSTRACT

High intensity focused ultrasound (HIFU) has many applications ranging from thermal ablation of cancer to hemostasis. Although focused ultrasound can seal a bleeding site, physical mechanism of acoustic hemostasis is not fully understood yet. To understand better the interaction between different physical mechanisms involved in hemostasis a mathematical model for acoustic hemostasis is developed. This model comprises the nonlinear Westervelt equation and the bioheat equations in tissue and blood vessel. In a three dimensional domain, the nonlinear hemodynamic equations are coupled with the acoustic and thermal equations. Convective cooling and acoustic streaming effects are incorporated in the modeling study. Effect of acoustic streaming on the blood flow out of the wound has been studied for two wound shapes and different sonication angles. It was theoretically shown that if focused ultrasound beam is applied directly to the bleeding site, the flow out of the wound can be reduced due to the acoustic streaming effect. Bleeding can be completely stopped even for a big wound, if the focal point location, ultrasound power and sonication angle are appropriately chosen. The sonication angles should be chosen in the range between 45° and 90°. The temperature around 70 °C can be achieved within a second on the blood vessel wall, thus showing the theoretical possibility of sealing the bleeding site by focused ultrasound.

1. Introduction

Bleeding is one of the major causes of death after traumatic injuries [1]. Management of this type of injuries in 1987 in the USA, for example, accounted for $64.7 billion (in 1993 dollars) [2,3]. Hemorrhage is stopped by vessel ligation, clamping, and repair of the vessel [4,5].

Acoustic hemostasis is a new field of ultrasound research. Focused ultrasound has been successfully applied to the treatment of tumors in different areas of the bodies, including the breast, prostate, uterine fibroids and liver [6,7]. Other promising applications of high intensity focused ultrasound (HIFU) include small blood vessel occlusion [8–11], hemostasis of bleeding vessels and organs [12–14]. In the latter case, the vessel wall aperture must be closed without affecting the vascular lumen to obviate both local and remote occlusions following the detachment of a blood

* Corresponding authors at: National Health Research Institutes, Institute of Biomedical Engineering and Nanomedicine, No. 35, Keyan Road, Zhunan, Taiwan and Department of Engineering Science and Ocean Engineering, National Taiwan University, Taiwan.
E-mail addresses: solovchuk@gmail.com (M.A. Solovchuk), twhsheu@ntu.edu.tw (T.W.H. Sheu).

http://dx.doi.org/10.1016/j.applthermaleng.2017.06.040
1359-4311/

Nomenclature

c_0	speed of ultrasound in tissue, m/s
c_i	small signal sound speed increment, m/s
c	specific heat, J/kg °C
f	ultrasonic frequency, Hz
$\underline{\mathbf{F}}$	force vector per unit volume, N/m^3
k	wave number
k_t	thermal conductivity of tissue, W/m °C
I	sound intensity, W/m^2
p	acoustic pressure, N/m^2
$\mathbf{P}$	fluid static pressure, N/m^2
q	ultrasound power deposition, W/m^3
t	time, s
T	temperature, °C
u	blood flow velocity, m/s
w	velocity in z direction, m/s
w_b	blood perfusion rate, kg/m^3 s
x	coordinate in the x direction
y	coordinate in the y direction
z	coordinate in the z direction

Greek symbols

α	absorption coefficient, Np/MHz m
β	nonlinearity coefficient
δ	acoustic diffusivity
λ	wavelength, m
μ	shear viscosity of blood flow, kg/m s
ρ	density, kg/m^3
ω	angular frequency, Hz
τ	relaxation time, s

Subscripts

t	tissue
b	blood

clot fragment by hemodynamic force and its blockage in a downstream vessel of smaller caliber. Therefore, the position of the ultrasound focal point represents a critical aspect of acoustic hemostasis. The ultrasound beam orientation and heating volume must be carefully selected to avoid appearance of any intraluminal thrombus. Moreover, this technique is only suitable to superficial vessels.

Acoustic hemostasis is mainly studied experimentally. However, the optimal strategy for the acoustic hemostasis remains to be defined. The ultrasound frequency and intensity, exposure duration, location of the focal point differ according to studies. The focus can be either fixed at the center of the wound or at its proximal or distal region. Ultrasound focus can be moved continuously throughout the wound. Sonication at a set of selected points can be also carried out.

Several studies are related to punctured blood vessel [1,13,15]. Under the same ultrasound parameters, the treatment time can differ even by an order of magnitude for similar punctures [15]. The difference can be attributed to the wound shape and the HIFU guidance. The ultrasound beam should be precisely located on the wound. If the location of the focal point is not properly determined, the exposure time needs to be highly increased for the same efficiency. In addition, physical processes should be well understood to improve the treatment planning.

Acoustic hemostasis was also investigated numerically [16,17]. Linear acoustic model was considered by the authors. However, for high ultrasound powers and large peak pressures used in acoustic hemostasis, this assumption is not valid. At high intensities nonlinear wave propagation effects become important. Nonlinear propagation effects can enhance the local heating by several times [18,19]. Therefore in the current work nonlinear acoustic model is considered. In Ref. [16], ultrasound propagation through different coupling materials between the biological tissues and transducer during acoustic hemostasis was studied numerically. Heating in homogeneous media was considered. The temperature increase was modeled using the classical Pennes bioheat equation [20]. The amount of the dissipated heat was estimated by averaging the effect of blood perfusion over all tissues. Focused ultrasound is able to produce hemostasis [1,13,15] in large blood vessels up to 10 mm. For tissues with large blood vessels (diameters larger than 0.5 mm) Pennes bioheat equation is not valid and convective blood flow cooling needs to be taken into account. Recently, a three-dimensional studies pointed out the influence of blood flow and acoustic streaming on the temperature distribution [18,21]. The proposed model was applied to get the temperature elevation in liver tumor in a patient-specific geometry [22]. In the present paper the developed mathematical model is applied to the acoustic hemostasis. Importance on the thermal and acoustic streaming effects will be addressed.

According to acoustic hemostasis experiments [13,15,23], the thermal effect exerted by focused ultrasound triggers hemostasis. The absorbed ultrasound energy in tissues is transformed into thermal energy. The resulting temperature elevation can soar up to 70 °C in about 1 s [13], thereby allowing sealing of the bleeding site. Blood flow at the wound can in theory carry away a part of the deposited energy. In the experiments [15], when the puncture site was exposed to air, a blood jet that appeared from the arterial injury was stopped upon exposure of focused ultrasound. In most experimental studies, ultrasound beam is oriented roughly perpendicularly to the wound. In the present paper several sonication angles and two wound shapes were studied. Sonication angle and focal point location can be optimized for bleeding arrest to reduce tissue damage and prevent thrombus risk.

2. Methods

The schematic of acoustic hemostasis treatment is presented in Fig. 1. Focused ultrasound device is located outside of the body.

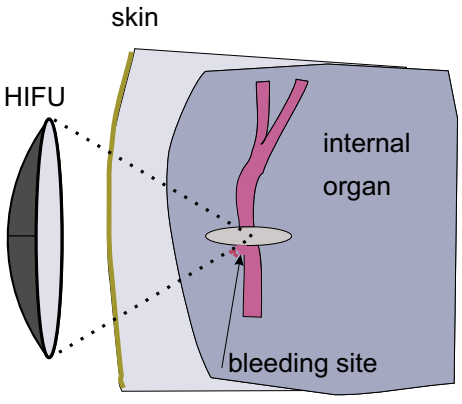

Fig. 1. The schematic of acoustic hemostasis treatment.

There is a water layer between the transducer and the skin. Ultrasound beam is focused at the bleeding site. Ultrasound energy can be transformed into thermal energy and the temperature at the focal area can be increased, which can help to seal the bleeding site. Focused ultrasound can also induce some additional flow motion (the effect is called acoustic streaming). Experimental studies showed that acoustic streaming can sufficiently reduce or even stop the blood flow out of the wound. However this effect is not very well understood. In this paper we are going to study numerically how acoustic streaming effect can change the blood flow motion out of the wound. For the construction of the mathematical model for acoustic hemostasis it is necessary to describe acoustic field to compute the pressure and thermal fields to calculate the temperature in tissue and blood vessel, and hydrodynamic field to estimate how acoustic field changes the blood flow velocity.

The three-dimensional (3D) acoustic-thermal-hydrodynamic coupling model has been proposed to compute the pressure, temperature, and blood flow velocity [18]. The mathematical model [18,21] relies on the coupling of: (1) nonlinear Westervelt equation with relaxation effects being taken into account; (2) heat equations in biological tissues; and (3) acoustic streaming-induced hydrodynamic equations.

2.1. Nonlinear acoustic equation

Acoustic field generated by a HIFU source was modeled using the coupled system of two partial differential equations given below [18]

$$\begin{aligned} &\nabla^2 p - \frac{1}{c_0^2}\frac{\partial^2 p}{\partial t^2} + \frac{\delta}{c_0^4}\frac{\partial^3 p}{\partial t^3} + \frac{\beta}{\rho_0 c_0^4}\frac{\partial^2 p^2}{\partial t^2} + \sum_i P_i = 0 \\ &\left(1 + \tau_i \frac{\partial}{\partial t}\right) P_i = \frac{2}{c_0^3} c_i \tau_i \frac{\partial^3 p}{\partial t^3} \end{aligned} \tag{1}$$

The above system of equations takes into account the effects of diffraction, absorption, nonlinear propagation and relaxation. In the above, p is the sound pressure, $\beta = 1 + \frac{B}{2A}$ the coefficient of nonlinearity, and δ the diffusivity of sound originating from fluid viscosity and heat conduction, τ_i the relaxation time and c_i the small signal sound speed increment for the i-th relaxation process. The first four terms in the first equation of the system (1) represent the classical Westervelt equation [24]. The new auxiliary variable P_i is included to model the relaxation processes. In the present paper two relaxation processes ($i = 2$) were considered.

For the linear acoustic equation the intensity is equal to $I_L = p^2/2\rho c_0$. For the nonlinear case the total intensity is $I = \sum_{n=1}^{\infty} I_n$, where I_n are the corresponding intensities for the respective harmonics nf_0. The ultrasound power deposition per unit volume is calculated by

$$q = \sum_{n=1}^{\infty} 2\alpha(nf_0) I_n \tag{2}$$

The absorption coefficient in tissue α obeys the following frequency law $\alpha = \alpha_0 (f/f_0)^{\eta}$, where $\alpha_0 = 8.1$ Np/m, $\eta = 1.0$ and $f_0 = 1$ MHz [25]. The unknown relaxation parameters τ_i, c_i in the differential system (1) were calculated through the minimization of a mean square error between the linear attenuation law and the relaxation model [18].

2.2. Radiation force and acoustic streaming hydrodynamic equations

Acoustic wave propagation in a medium exerts a force acting in the direction of propagation, which is called the radiation force. It can be defined as a period averaged force acting on the medium by a sound wave. Under the linear acoustic propagation assumption, this average force is equal to zero. So the radiation force represents the second order nonlinear effects. Several mechanisms can contribute to the generation of this force, including reflection/scattering at the interfaces, change of ultrasound energy during the propagation due to the absorption and scattering [26]. Radiation force can be used to access elastic tissue properties, for biomedical diagnostic applications, drug and gene delivery [27]. Good review about biomedical applications of radiation force can be found in [26,28].

While ultrasound wave is propagating in the liquid, the liquid starts moving in the direction of propagation and acoustic streaming appears. In the present study we are going to investigate how the acoustic streaming effect can help to stop the bleeding. During acoustic hemostasis in order to seal the bleeding site, first it is necessary to reduce the flow out of the wound. Vaezy et al. [14] experimentally showed that radiation force, generated by the focused ultrasound device, was able to temporarily stop the bleeding in the open wound. Blood jet from the puncture was stopped upon the exposure of focused ultrasound. The ultrasound beam was perpendicular to the blood vessel and was focused on the puncture in the artery. It was shown that it was easier to produce hemostasis when the blood was pushed back by streaming. However, the treatment time can differ by the order of magnitude for similar punctures, ranging from ten to one hundred seconds [1,29]. The difference can be attributed to the wound shape, focal point location, beam orientation and ultrasound guidance. Most of the experimental studies considered the perpendicular orientation of blood vessel and the ultrasound beam. In order to optimize the treatment, theoretical understanding of the acoustic streaming effect on the flow out of the wound is necessary. Different sonication angles, focal point locations and wound shapes will be studied in the present paper. It will be shown that these parameters can be optimized during acoustic hemostasis. In the following sections we will show that even for the big wound with the length of 6 mm, the bleeding can be completely stopped by the acoustic streaming effect, while without applying focused ultrasound about 90% of mass flow comes out of the wound.

One of the first studies about acoustics streaming has been performed by Rayleigh [30], who studied circulation of air in Kundt's tubes. Later theoretical studies on the prediction of streaming either in the tube or in the open domain have been performed by Eckart [31], Nyborg [24,32] and Tjotta [33]. Simple analytical expression exists for the estimation of the streaming velocity in a plane progressive wave [33]:

$$v = (2\alpha I/c_0\mu)(2a)^2 G,$$

where v is the streaming velocity, μ the viscosity of the medium, $2a$ the ultrasound beam width and G a geometric factor dependent on the geometry of the problem. However, this analytical expression can be only applied for weakly focused transducers under linear acoustic approximation. However, at high intensities and at complex geometries nonlinear hydrodynamic equations should be solved.

In this study the flow in large blood vessels is assumed to be incompressible and laminar, for which the mass conservation equation has the form $\nabla \cdot \underline{\mathbf{u}} = 0$. The equation for modeling the blood flow motion with the acoustic streaming effect being taken into account is as follows [34,35,36]

$$\frac{\partial \underline{\mathbf{u}}}{\partial t} + (\underline{\mathbf{u}} \cdot \nabla)\underline{\mathbf{u}} = \frac{\mu}{\rho}\nabla^2 \underline{\mathbf{u}} - \frac{1}{\rho}\nabla \mathbf{P} + \frac{1}{\rho}\underline{\mathbf{F}} \tag{3}$$

In the above, $\mathbf{P}$ is the static pressure, μ (=0.0035 kg/m s) the shear viscosity of blood flow, and ρ the blood density. In Eq. (3), the radiation force vector $\underline{\mathbf{F}}$ is assumed to act along the acoustic axis $\underline{\mathbf{n}}$ and it has the following form [24]

$$\underline{\mathbf{F}} \cdot \underline{\mathbf{n}} = -\frac{1}{c_0}\nabla \vec{I} = \frac{q}{c_0} \tag{4}$$

Gravity is known to significantly influence pulmonary blood flow distribution according to the height and hence the ventilation-perfusion ratio [37]. It also impacts the cerebral venous flow and the venous return in the inferior limbs in the standing position, hence resulting in the presence of valves to counter backflow during muscular contraction of leg skeletal muscles. In the present paper, the subject under consideration is in the lying position. Body forces, such as gravity and electromagnetic field, during MRI, can nevertheless be easily added to the model.

2.3. Energy equation for tissue heating

In the current simulation study of thermal field the physical domain has been split into two subdomains for the perfused tissue and the flowing blood. In a region free of large blood vessels, the classical Pennes bioheat equation [20] given below is employed to model the transfer of heat in the perfused tissue region

$$\rho_t c_t \frac{\partial T}{\partial t} = k_t \nabla^2 T - w_b c_b (T - T_a) + q \tag{5}$$

In the above bioheat equation ρ, c, k denote the density, specific heat, and thermal conductivity, respectively. The subscripts t and b refer to the tissue and blood domains. The notation T_a denotes the arterial temperature. The variable w_b ($\equiv$0.5 kg/m^3 s) in Eq. (5) is the perfusion rate for the tissue cooling in capillary flows.

In the region inside the blood vessel, temperature rise was calculated by solving the following heat equation

$$\rho_b c_b \frac{\partial T}{\partial t} = k_b \nabla^2 T - \rho_b c_b \underline{\mathbf{u}} \cdot \nabla T + q \tag{6}$$

where $\underline{\mathbf{u}}$ is the blood flow velocity. In the above equation the biologically relevant heat source, which is q, and the heat sink, which is $-\rho_b c_b \underline{\mathbf{u}} \cdot \nabla T$, are added to the conventional diffusion-type heat equation. It is noted here that the above thermal Eqs. (5) and (6) are coupled with the acoustic Eq. (1) for the acoustic pressure through the power deposition term q defined in Eq. (2). In order to calculate the blood flow velocity $\underline{\mathbf{u}}$, shown on the right hand side of Eq. (6), in a three dimensional geometry hydrodynamic equations given in Eq. (3) should be solved. Focused ultrasound can induce an additional mass flow in a fluid (acoustic streaming). The cooling due to blood flow motion and acoustic streaming effect will be taken into account. In Ref. [18] it was shown that in the high-intensity regime acoustic streaming velocity magnitude can be 3–30 times larger than the velocity in a blood vessel. Large velocity gradients can be generated near the blood vessel wall, thereby leading to large shear stresses. The large shear stresses may cause damage of the vessel wall cells. Several experimental studies [38,39] showed that the walls of the blood vessels were sometimes damaged after ultrasound irradiation at high powers.

2.4. Solution procedures and description of the problem

The nonlinear system of acoustic Eq. (1) is solved by the implicit finite difference time domain method presented in [18]. The second order accurate scheme in time and sixth order accurate scheme in space are implemented for the solution of the system (1). Discretization of this system of differential equations is started with the approximation of the temporal derivative $\frac{\partial}{\partial t} P_i^{n+1}$ shown in the second equation of the system (1):

$$\frac{\partial}{\partial t} P_i^{n+1} = \frac{1}{2\Delta t}(3P_i^{n+1} - 4P_i^n + P_i^{n-1}) \tag{7}$$

After some algebraic manipulation the second equation in the system (1) can be rewritten in the form as:

$$P_i^{n+1} = \frac{2}{c_0^3}\frac{c_i \tau_i}{1 + 1.5\tau_i/\Delta t}\frac{\partial^3 p^{n+1}}{\partial t^3} - \frac{\tau_i}{2\Delta t + 3\tau_i}(-4P_i^n + P_i^{n-1}) \tag{8}$$

The above P_i^{n+1} is then substituted into the first equation of the system (1).

Temporal derivatives in the first equation of the system (1) are approximated using the following second order accurate schemes:

$$\left.\frac{\partial^2 p}{\partial t^2}\right|^{n+1} = \frac{2p^{n+1} - 5p^n + 4p^{n-1} - p^{n-2}}{(\Delta t)^2} \tag{9}$$

$$\left.\frac{\partial^3 p}{\partial t^3}\right|^{n+1} = \frac{6p^{n+1} - 23p^n + 34p^{n-1} - 24p^{n-2} + 8p^{n-3} - p^{n-4}}{2(\Delta t)^3} \tag{10}$$

The nonlinear term $\frac{\partial^2 p^2}{\partial t^2}|^{n+1}$ is linearized using the second order accurate relation:

$$\begin{aligned}\left.\frac{\partial^2 p^2}{\partial t^2}\right|^{n+1} &= \frac{\partial}{\partial t}\left(\frac{\partial p^2}{\partial t}\right)\Bigg|^{n+1} \\ &= 2\frac{\partial}{\partial t}\left(p^n \left.\frac{\partial p}{\partial t}\right|^{n+1} + p^{n+1}\left.\frac{\partial p}{\partial t}\right|^{n} - p^n \left.\frac{\partial p}{\partial t}\right|^{n}\right) \\ &= 2\left(2p_t^n p_t^{n+1} + p^n p_{tt}^{n+1} + p^{n+1}p_{tt}^n - (p_t^n)^2 - p^n p_{tt}^n\right)\end{aligned} \tag{11}$$

The above temporal derivatives are then substituted into the system (1) to get the Helmholtz equation. Helmholz equation is solved implicitly using the three-point sixth-order accurate scheme [18]. Accuracy of the numerical solutions for acoustic pressure was examined in [18] by comparing them with the known analytical and numerical solutions obtained by other authors [40,41]. The predicted numerical results were also in good agreement with the experimental data [18,21].

With the known acoustic pressure, the ultrasound power deposition in Eq. (2) and the acoustic streaming force in Eq. (4) were calculated. The acoustic streaming force was then substituted into Eq. (3) to compute blood flow velocity. Afterwards, temperatures in blood flow domain and in tissue were calculated. The initial temperature is equal to 37 °C. Finite-volume method has been applied for the analysis of the three-dimensional problem. A detailed description of the solution procedures can be found in our previous articles [18,21,35]. The computational model for the calculation of acoustic streaming velocity was validated by comparing the results with those of Kamakura et al. [36]. For the validation of the computational model for the thermal field, with and without flow, the predicted results were compared with the experimental results of Huang et al. [42]. Good agreement between the predicted and measured temperatures with and without flow has been found [42] as it can be seen in Fig. 2. We have also performed MRI measurements of temperature increase during focused ultrasound treatment in ex-vivo porcine muscle [43]. Excellent agreement between our numerical simulation results and experimental data has been found [43].

As we mentioned before, two main mechanisms of acoustic hemostasis are considered in this paper: the stopping of the blood flow out of the wound due to the radiation force (acoustic streaming effect) and sealing of the wound by high temperature. In order to investigate the effect of acoustic streaming on the blood flow out of the wound, we are going to consider two different wound geometries. Two wound shapes, namely, the small circular wound with a diameter of 2 mm and a big long wound of 6 mm in length and 2 mm in width will be investigated as it can be seen in Fig. 3. In the present paper the vessel with a diameter of 3 mm is

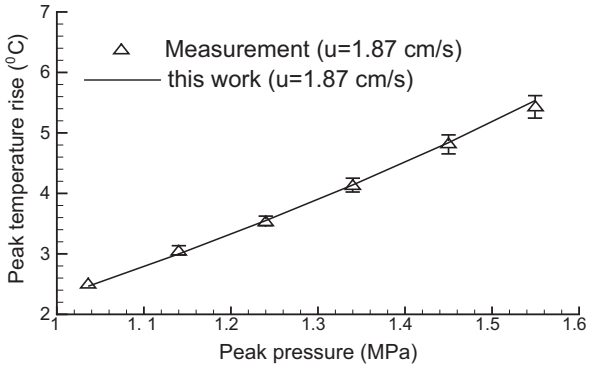

Fig. 2. The comparison of the predicted results for the temperature rise at the focus with the experimental results of Huang et al. [42] as function of focal pressure. The focus was located 0.4 mm away from the vessel wall in a phantom, vessel is parallel to the acoustic axis and flow velocity is 1.87 cm/s.

considered. The fully developed velocity profile is prescribed at the inlet of blood vessel, while zero gradient velocity boundary condition is applied on the outlet plane. The pressure at the wound is equal to the tissue pressure. At vessel inlet, the blood flow cross-sectional average velocities are set at 0.016 m/s and 0.13 m/s. These imposed velocities correspond to the velocities in veins and arteries with the diameter of 3 mm [44].

Unstructured mesh has been generated for the study of flow in the vessel with the wound. The number of tetrahedral elements varied from 191,000 to 207,000 elements for the vessel with the small and big wounds correspondingly. Mesh independence study has been performed. The difference of the predicted velocity fields using the current mesh and the refined mesh (by increasing the number of elements by 50%) was less than 1%.

Thermal effect has been investigated for three different sonication angles (see Section 3.2). The vessel with a diameter 3 mm was considered. A structured mesh was used in both tissue and vessel domain. The focal point was located on the blood vessel wall. Close to the blood vessel wall in the focal area the refined grids were generated with a mesh size of 0.15 mm $*$ 0.15 mm $*$ 0.2 mm. In the focal area (4 mm $*$ 4 mm $*$ 15 mm) the grid with a mesh size of 0.2 $*$ 0.2 $*$ 0.2 was used. The number of hexahedral elements varied from 512,000 to 621,000 for different blood vessel orientations. Mesh independence study was performed by comparing the predicted results using the current mesh and the refined mesh with the increased number of the elements by 50%. The predicted difference for the velocity and temperature fields using two different meshes was less than 1%.

The single element HIFU transducer used in this study is spherically focused with an aperture of 12 cm and a focal length of 12 cm. In this study, the transducer with the frequency $f_0 = 1.0$ MHz is considered. Focal intensity is 2240 W/cm^2. Peak positive and negative pressures are $P_+ = 14$ MPa and $P_- = 6.4$ MPa (in linear approximation $P_{lin} = 8.5$ MPa), respectively, and the sonication time is 0.6 s. The parameters used in the current simulation are listed in Table 1 [25].

3. Results and discussion

As it was already mentioned in introduction section, heating is considered as one of the main consequences during acoustic hemostasis. Increase of the temperature above a certain value allows cauterizing of the bleeding site. The temperature of 70 °C can be assumed as the threshold temperature for the acoustic hemostasis [13]. However, blood flow out of the wound may carry away heat at the bleeding site and it can significantly reduce the temperature at the bleeding site. Blood also has a lower absorption than a tissue. For example, in Table 1 it can be seen that absorption coefficients of liver tissue and blood differ by about five times. Therefore if blood is still flowing out of the wound it is quite difficult to seal the wound. First of all, it is necessary to reduce or stop the flow out of the wound, then thermal energy can be applied to cauterize the bleeding site and seal the wound. In the experiments [15] with the wound exposed to air it was shown that blood flow out of the wound can be stopped after applying focused ultrasound energy to the bleeding site. Focused ultrasound induces streaming of the blood away from the focus of the transducer. This effect is called acoustic streaming. Thus, physical processes involved in acoustic hemostasis can be described in the following way: first, acoustic streaming effect reduces or stops the flow out of the wound, afterwards thermal effect is used to seal the wound. In the following section we are going to investigate numerically the acoustic streaming effect for the two wound shapes under investigation and different sonication angles and thermal effect for different sonication angles.

3.1. Importance of acoustic streaming

3.1.1. Bleeding in a small circular wound

In the previous studies [18,21] it was shown that focused ultrasound can induce acoustic streaming velocities up to 100 cm/s in

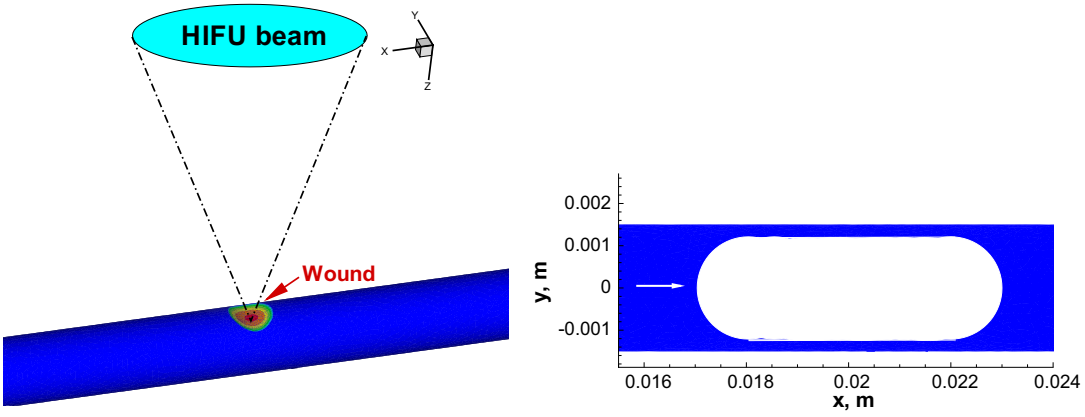

(a) (b)

Fig. 3. Schematic of the problem. (a) a small circular wound with the diameter 2 mm in the blood vessel ($d = 3$ mm); (b) a big wound with the length 6 mm and the width 2 mm. The blood vessel diameter is $d = 3$ mm.

Table 1
Acoustic and thermal properties for the tissue and blood.

Tissue	c_0 $\left(\frac{m}{s}\right)$	ρ $\left(\frac{kg}{m^3}\right)$	c $\left(\frac{J}{kg\,K}\right)$	k $\left(\frac{W}{mK}\right)$	α $\left(\frac{Np}{m}\right)$
Tissue	1540	1055	3600	0.512	$8.1f$
Blood	1540	1060	3770	0.53	$1.5f$

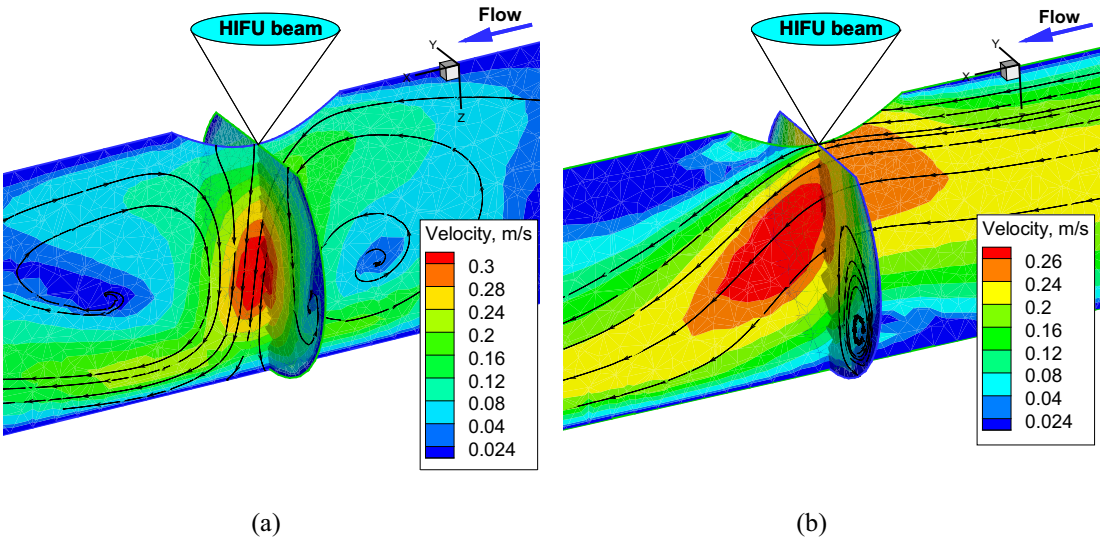

(a) (b)

Fig. 4. The predicted velocity (m/s) in vein (a) and artery (b) when the acoustic streaming effect is taken into account.

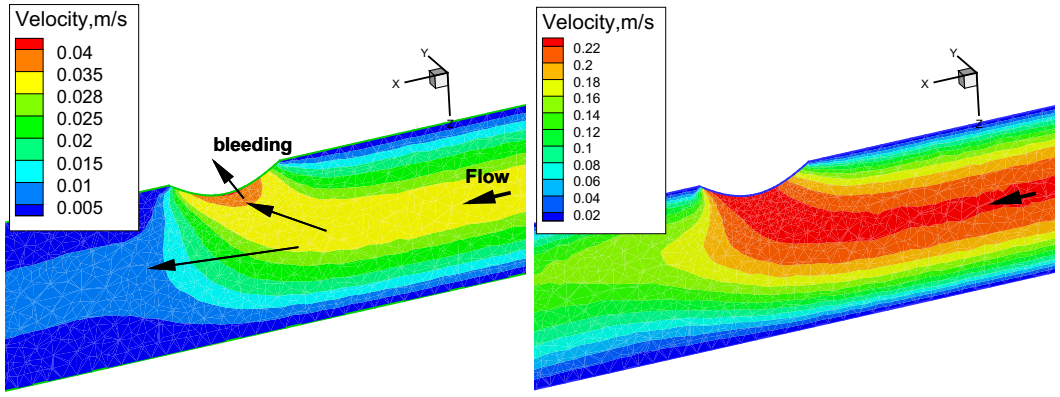

(a) (b)

Fig. 5. The predicted velocity (m/s) in vein (a) and artery (b) without considering acoustic streaming effect.

the blood vessel and can affect the ultrasound heating. When blood vessel was placed perpendicularly to the acoustic axis, acoustic streaming velocity magnitude becomes smaller comparing with that of the parallel blood vessel orientation.

When the focus of HIFU transducer is directed towards a bleeding site, the local absorption of acoustic energy supplies an extra momentum to the fluid and this force can result in streaming of the blood in the direction away from the focus of transducer. Usually in the acoustic hemostasis experiments blood vessel was located perpendicularly to the acoustic axis. However it is not very clear what blood vessel orientation is the optimal one. For the case of big wound focal point locations and scanning paths can be planned differently. We are therefore motivated to investigate the effects of blood vessel orientation (sonication angle) and focal point location.

Let's consider a hole (wound) on the blood vessel wall. The diameter of this hole is 2 mm. The diameter of the blood vessel is 3 mm, and the maximum velocities are 3.2 cm/s (vein) and 26 cm/s (artery). Acoustic streaming velocity magnitude is 30 cm/s (without acoustic streaming the maximum velocity in the vein is 3 cm/s). Acoustic streaming velocity magnitude is one order of magnitude larger than the blood flow velocity in the vein.

In Figs. 4 and 5 the velocity profiles in vein and artery are presented with and without incident focused ultrasound. In Tables 2 and 3 mass flow rates at the inlet and two outlets (outlet and wound) are presented in the vein and in the artery. Mass flow rate

Table 2
Acoustic streaming effect on the mass flow rate in the small wound in the vein ($u = 1.6$ cm/s).

Mass flow rate	Outlet	Wound	Inlet
Without AS	22%	78%	100%
With AS	100%	0	100%

Table 3
Acoustic streaming effect on the mass flow rate in the small wound in the artery ($u = 13$ cm/s).

Mass flow rate	Outlet	Wound	Inlet
Without AS	55%	45%	100%
With AS	71%	29%	100%

Table 4
The effect of acoustic streaming on the mass flow rate in the big wound in the vein ($u = 1.6$ cm/s).

Mass flow rate	Outlet	Wound	Inlet
Without AS	**3**%	97%	100%
With AS	100%	0	100%

Table 5
The effect of acoustic streaming on the mass flow rate in the big wound in the artery ($u = 13$ cm/s).

Mass flow rate	Outlet	Wound	Inlet
Without AS	26%	74%	100%
With AS	47%	53%	100%

through the surface S is calculated by $\iint_S \rho \vec{u}\, \vec{dS}$, i.e. the flow of mass m through a surface per unit time t. Mass flow rate at the vessel inlet is equal to 100%. Without AS, 78% of the total mass flow comes out of the wound. If we switch the transducer, radiation force will cause the acoustic streaming flow to occur. With the acoustic streaming effect being taken into account, the bleeding in the vein can be completely stopped. However, there is still a small bleeding out of the artery. In the artery the blood flow out of the wound can be reduced by an amount from 45% to 29%. In order to stop blood flow out of the wound, higher power depositions should be considered.

Simulations show that acoustic streaming velocity profile reaches the steady state within a very short time interval of 0.12 s, within which bleeding can be stopped or sufficiently reduced. This prediction is in agreement with the experimental observations [15,45–47]. Since the acoustic streaming velocity can reach steady state within a very short time, only steady state velocity contours in the present paper are plotted, unless otherwise stated.

In the next section we will show that under different sonication angles blood flow can be stopped even in the artery.

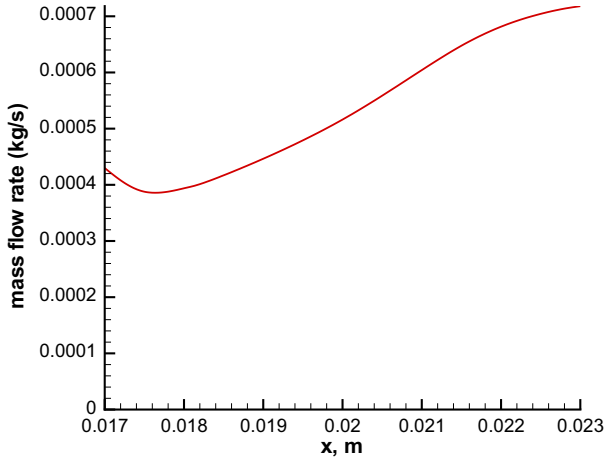

Fig. 7. The predicted mass flow rate (kg/s) at the big wound for the cases with different focal point locations, artery case.

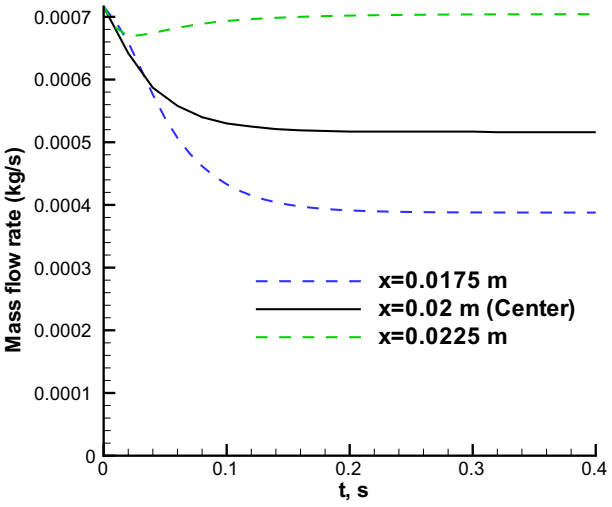

Fig. 8. The predicted mass flow rate (kg/s) with respect to time in the wound for the cases with different focal point locations, artery case.

3.1.2. Bleeding in a big wound

In Tables 4 and 5 mass flow rates at the inlet and two outlets of the blood vessel with a big wound are presented for the cases with and without considering acoustic streaming effect. The focal point is located at the center of the wound. For a larger wound case it is more difficult to stop bleeding. When we take into account the acoustic streaming effect the bleeding out of the wound in the vein can be stopped. However, there is still a flow of blood out of the wound in the artery. The blood flow out of the wound in the artery is reduced from 74% to 53% of the total mass flow due to the acoustic streaming effect. In Fig. 6 velocity profiles in the artery are

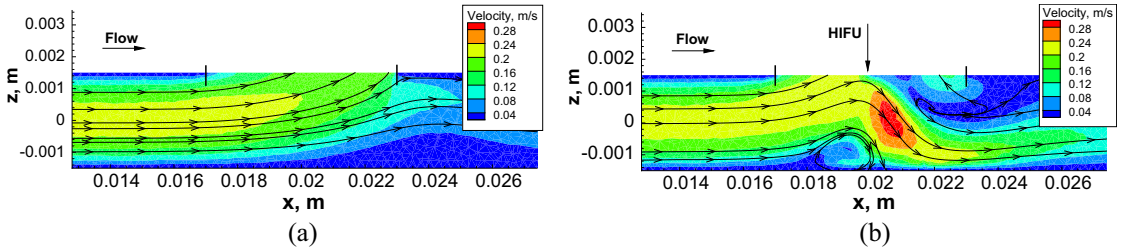

Fig. 6. The predicted velocity magnitude (m/s) contours in the artery with the big wound for the cases with (right) and without (left) considering acoustic streaming.

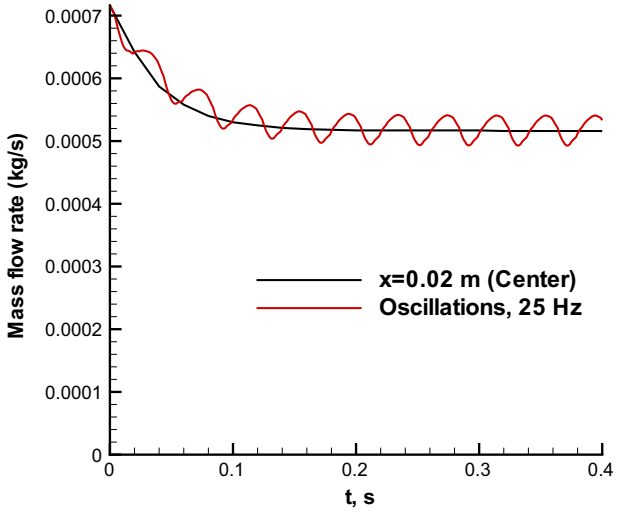

Fig. 9. The predicted mass flow rate (kg/s) with respect to time in the big wound for two cases: (1) focal point is located at the center of the wound ($x = 0.02$) and (2) focal point is oscillating around the center of the wound with the frequency 25 Hz.

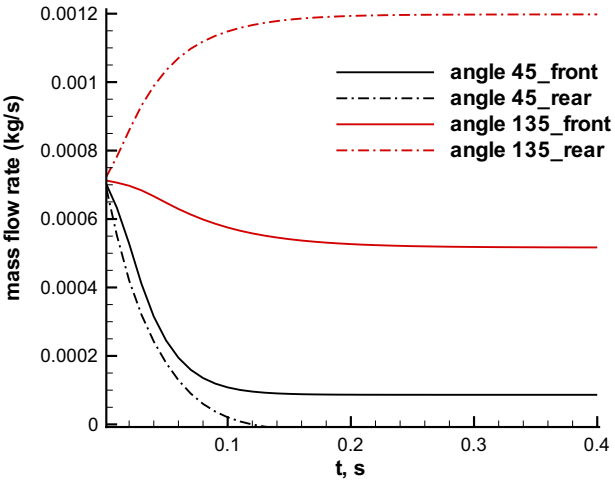

Fig. 12. The predicted mass flow rates (kg/s) with respect to time in the big wound for the cases with different sonication angles and different locations of the focal point in the artery.

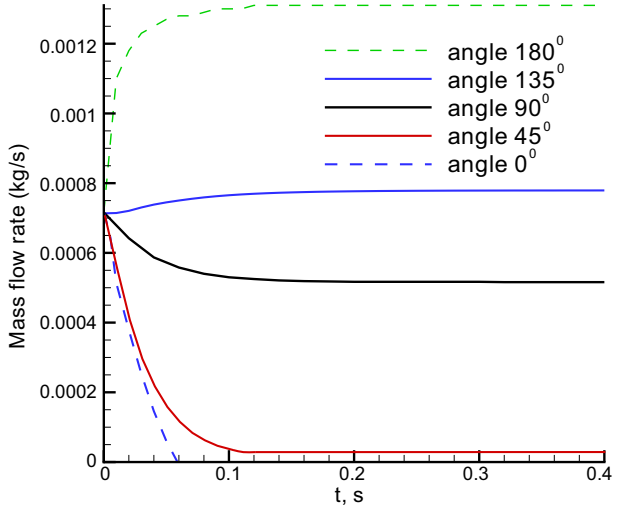

Fig. 10. The predicted mass flow rate (kg/s) with respect to time in the big wound for the cases with different sonication angles in the artery.

presented for the cases with and without focused ultrasound. It can be seen that bleeding is stopped in the small focal area. This means that in the focal area we can seal the bleeding site by heating.

In Fig. 7 mass flow rate out of the wound is presented as the function of focal point location along the axis of the big wound. When the focal point is located at the rear of the wound, the largest mass flux and consequently the largest bleeding occur. When the focal point is located close to the front of the wound ($x = 0.0175$), the mass flux is minimal. Therefore to reduce the bleeding in the large wound, focal point should be located in front of the wound. In Fig. 8 mass flow rate out of the wound is presented with respect to time at different focal point locations. Within 0.12 s blood flow becomes steady. The smallest mass flow rate occurs at the condition when the focal point is located at the front of the wound. The worst case happens when the focal point is located at the rear of the wound.

Several ways of ultrasound sonications can be applied to stop bleeding in the wound. In the work of [12] mechanical scanning of HIFU probe was used to stop bleeding in a punctured artery. The frequency of the scanning was 15 or 25 Hz, the amplitude of the scanning was equal to the length of the wound (5–10 mm). In Fig. 9 the predicted evolution of the mass flow rate for the case

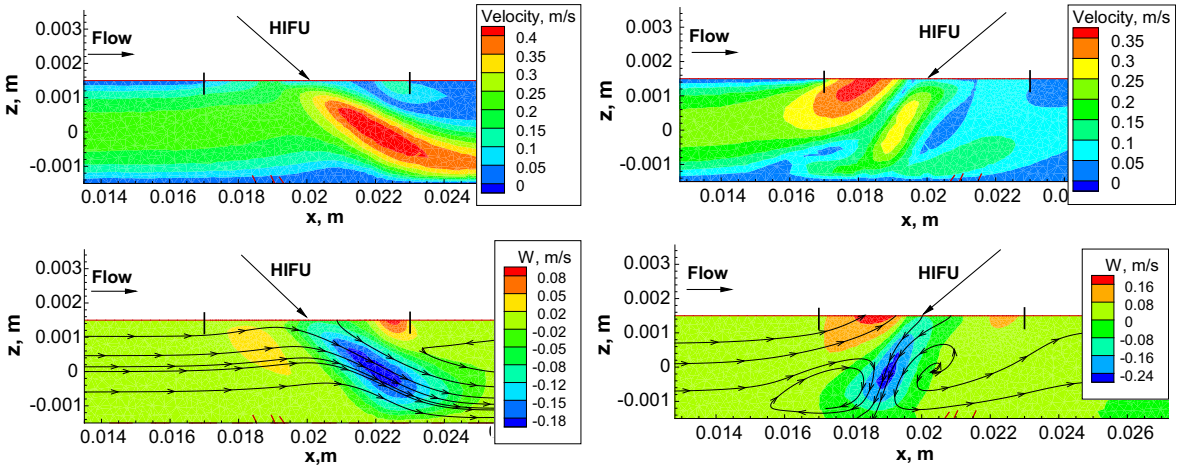

Fig. 11. The predicted velocity magnitude (m/s) contours (a and b) and stream lines (c and d) in the artery with the big wound for the sonication angles 45° and 135°. Focal point is located at the center of the wound in the artery. w - velocity component in z direction.

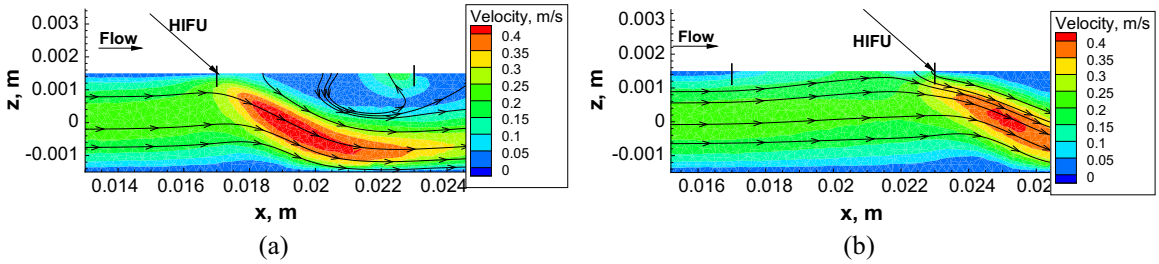

Fig. 13. The predicted velocity magnitude (m/s) in the artery with the big wound for the cases with different locations of the focal point: (a) in front of the wound and (b) at the rear of the wound. The sonication angle is 45°.

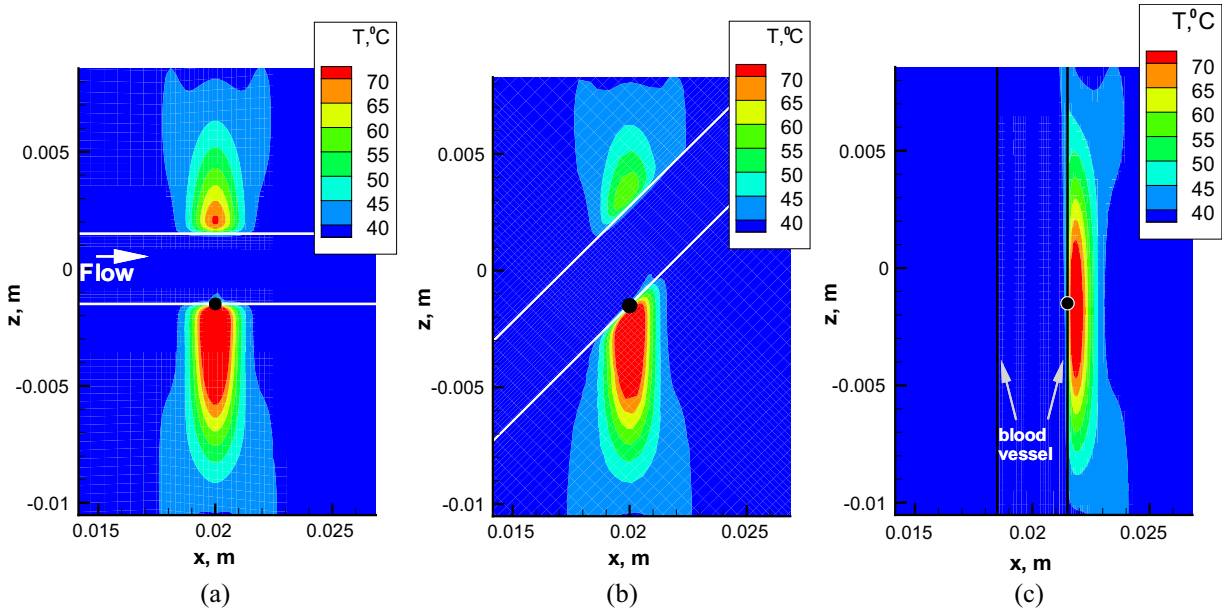

Fig. 14. The predicted temperature contours at $t = 0.6$ s at the cutting plane $y = 0$ for different sonication angles 90° (a), 45° (b) and 0° (c). Focal point (•) is located on the blood vessel wall.

of big wound is presented for the case of mechanical scanning of HIFU beam along the wound. Focal point was oscillating around the center of the wound with the frequency 25 Hz. We can see that mass flow rate is oscillating around the value of mass flow obtained at the central location of focal point. Decrease of the oscillating frequency will lead to the increased oscillating amplitude. The mass flow rate is very close to that of the case when the focal point is at the center of the wound.

3.1.3. Bleeding in a big wound. Different sonication angles

In Fig. 10 the evolution of the predicted mass flow out of the big wound is presented for different sonication angles in the artery. Focal point is located at the center of the wound. Better sonication angles range from 0° to 90°. At the angle 0° it's possible to completely stop bleeding within 0.1 s. Because ultrasound beam is quite narrow, for 0° sonication it's quite difficult to allocate the ultrasound beam precisely on the wound. For the sonication angle 45° there is only a small bleeding at the rear of the wound (Fig. 11). In the experiments, 90° sonication was mostly used. From the simulation point of view, it is better to use 45°. The predicted velocity magnitudes in the artery with the big wound for two different sonication angles 45° and 135° are presented in Fig. 11. For 135° sonication there is a reverse flow near the center of the wound. This reverse flow acts like a dam and therefore the velocity magnitude in the beginning of the wound is increased. Comparison of the mass flow rates with and without AS for this sonication angle shows that 135° sonication increases bleeding and this angle should be avoided in the treatment.

In Fig. 12 the evolution of the predicted mass flow out of the big wound is presented for the two sonication angles 45° and 135° and two locations of the focal point: at a location in front of the wound and at the rear of the wound. The corresponding velocity magnitude for the sonication angle 45° can be seen in Fig. 13. When the focal point is located at the rear of the wound and the angle is 45°, bleeding can be stopped. When the focal point is located in front of the wound and the angle is 45°, there is still a small blood flow out of the wound at the rear of the wound. For 135° an opposite result is obtained. For 90° and 135° sonications focal point should be located at the front side of the wound. The present numerical simulations show that 135° sonication should be avoided, because in this case the degree of bleeding is increased. The smallest mass flow rate occurs at 45° sonication when the focal point is located at the rear of the wound. Sonication angles between 45° and 90° should be considered in order to reduce the flow out of the wound. In some cases flow out of the wound can be stopped.

Although in the experiments 90° sonications are mostly used [15], we have shown that for a big wound the optimal focal point location is at the rear of the wound and the optimal angle is 45°. In this case the flow out of the wound can be completely stopped. However the wound is not sealed yet, we should apply thermal energy in order to cauterize the bleeding site. In the following sec-

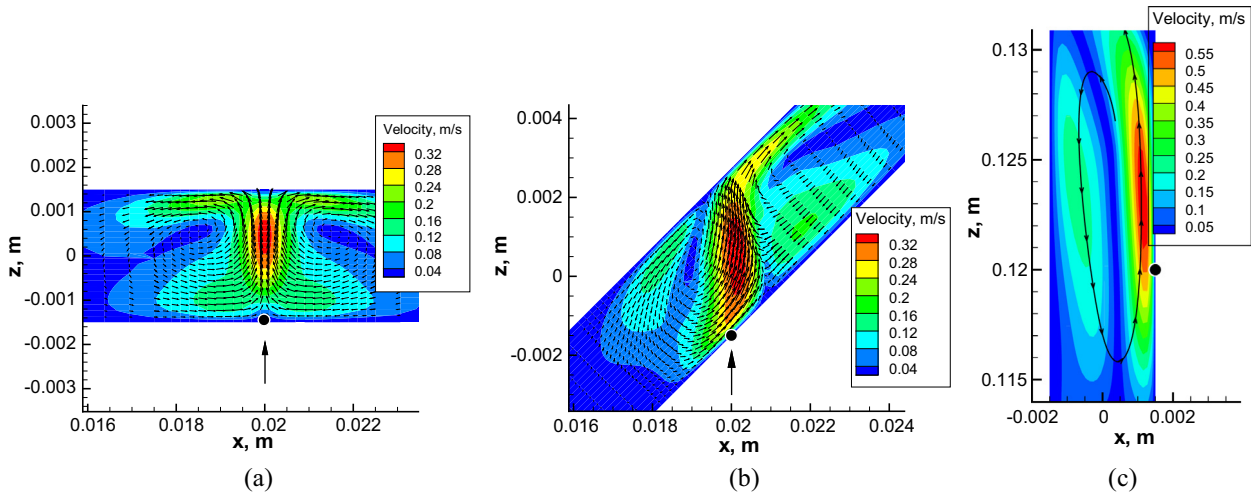

Fig. 15. The predicted acoustic streaming velocity vectors and the magnitudes contours at the cutting plane in the blood vessel without an externally applied flow (no blood flow) for different sonication angles (a) 90°; (b) 45°; (c) and 0°. Focal point (•) is located on the blood vessel wall.

tion we are going to investigate the thermal effect of ultrasound for different sonication angles.

3.2. Thermal effects

Let's study the temperature distribution in the tissue and in the blood domain during acoustic hemostasis. In most of the experimental studies ultrasound beam was located perpendicularly to the blood vessel. However, the optimal angle between the blood vessel and ultrasound beam is not very clear and it is not always possible to focus ultrasound beam perpendicular to the blood vessel. We are going to investigate how the sonication angle can affect the temperature elevation. We assumed that acoustic streaming effect has already stopped the flow out of the wound and the blood vessel is intact. Focal point is located on the blood vessel wall. Blood flow velocity in the vein is 1.6 cm/s. In Fig. 14 the predicted temperature contours at $t = 0.6$ s are presented at the cutting plane $y = 0$ for three different sonication angles. We can see a very small temperature increase inside the blood vessel.

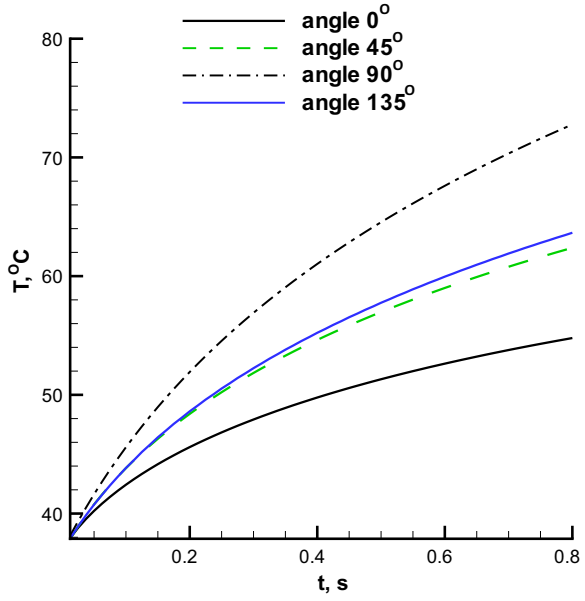

Fig. 16. The predicted temperature (°C) at the focal point as the function of time for different sonication angles.

The predicted acoustic streaming velocity at the cutting plane in the blood vessel without an externally applied flow is presented in Fig. 15 for three different sonication angles. The acoustic streaming velocity magnitudes are 34 cm/s, 36 cm/s and 60 cm/s for the sonication angles 90°, 45° (or 135°) and 0° (or 180°), respectively. The acoustic streaming velocity has the smallest value for 90° sonication and the largest value for 0° sonication. For all sonication angles, acoustic streaming velocity magnitude is up to an order of magnitude larger than the velocity in blood vessel (1.6 cm/s in vein and 13 cm/s in artery). Therefore cooling due to acoustic streaming effect can prevail over the blood flow cooling and can therefore represent the main cooling mechanism.

In Fig. 16 the predicted temperature is presented at the focal point as the function of time for different sonication angles. It can be seen that for 90° sonication the predicted temperature has the largest value and for 0° sonication the predicted temperature has the smallest value. For 45° and 135° sonications the predicted temperatures are almost the same (about 1 °C difference), because acoustic streaming velocity magnitude (35 cm/s) is an order of magnitude larger than the velocity in blood vessel (1.6 cm/s) and acoustic streaming is the main cooling mechanism in this case. The temperature around 70 °C on the blood vessel wall can be reached at $t = 0.6$ s for 90° sonication, for other sonication angles it will take a longer time to reach the temperature 70 °C. This shows the possibility to stop bleeding theoretically. For a smaller blood vessel the effects of blood flow cooling and acoustic streaming will be smaller.

In the current subsection we assumed that there is no blood flow coming out of the wound. In this case the temperature around 70 °C can be reached quite rapidly ($t < 1$ s) and the wound can be sealed within a short time period. Simulation shows that 90° sonication should be chosen in order to optimize the treatment.

4. Conclusions

The mathematical model for the simulation of acoustic hemostasis is proposed in the current paper. Our analysis is based on the nonlinear Westervelt equation with the relaxation effect being taken into account and the bioheat equations are applied in blood vessel and tissue domains. The nonlinear hemodynamic equation is also considered with the acoustic streaming effect being taken into account.

Both thermal and acoustic streaming effects have been investigated in the current paper. The importance of acoustic streaming was examined for different blood vessel orientations and focal point locations. Acoustic streaming velocity magnitude is up to 60 cm/s and this magnitude is several times larger than the velocity in blood vessel. If focused ultrasound beam is applied directly to the bleeding site, the flow out of a wound is considerably reduced due to acoustic streaming. Bleeding can be even completely stopped depending on the blood vessel orientation and the focal point location. As a result, the wound can be quickly sealed. Simulations show that the temperature around 70 °C can be reached within a second on the blood vessel wall, if there is no flow out of the wound. The temperature inside blood vessel remains almost unchanged. Sonication angles between 45° and 90° should be considered in order to reduce blood flow out of the wound. This simulation confirms the theoretical possibility of sealing the bleeding site by means of focused ultrasound. The blood vessel remains patent after the treatment.

Acknowledgement

The authors would like to acknowledge the financial support from the Center for Advanced Study in Theoretical Sciences and from the Ministry of Science and Technology, R.O.C., under the grant MOST-105-2221-E-400-005. This study was also supported by NHRI's project BN-104-PP-08.

References

[1] V. Zderic, A. Keshavarzi, M.L. Noble, M. Paun, S.R. Sharar, L.A. Crum, R.W. Martin, S. Vaezy, Hemorrhage control in arteries using high-intensity focused ultrasound: a survival study, Ultrasonics 44 (2006) 46–53.
[2] S. Vaezy, V. Zderic, Hemorrhage control using high intensity focused ultrasound, Int. J. Hypertherm. 23 (2007) 203–211.
[3] T.R. Miller, D.C. Lestina, Patterns in US medical expenditures and utilization for injury, 1987, Am. J. Public Health 86 (1996) 89–93.
[4] O.M. Austin, H.P. Redmond, P.E. Burke, P.A. Grace, H.B. Bouchier, Vascular trauma - a review, J. Am. Coll. Surg. 28 (1995) 59–70.
[5] M.O. Perry, Vascular trauma, Adv. Surgery 28 (1995) 59–70.
[6] Y.F. Zhou, High intensity focused ultrasound in clinical tumor ablation, World J. Clin. Oncol 2 (2011) 8–27.
[7] T.A. Leslie, J.E. Kennedy, High intensity focused ultrasound in the treatment of abdominal and gynaecological diseases, Int. J. Hypertherm. 23 (2007) 173–182.
[8] K. Hynynen, V. Colucci, A. Chung, F. Jolesz, Noninvasive arterial occlusion using MRI-guided focused ultrasound, Ultrasound Med. Biol. 22 (1996) 1071–1077.
[9] J. Serrone, H. Kocaeli, T. Douglas Mast, M.T. Burgess, M. Zuccarello, The potential applications of high-intensity focused ultrasound (HIFU) in vascular neurosurgery, J. Clin. Neurosci. 19 (2012) 214–221.
[10] P.W. Henderson, G.K. Lewis, N. Shaikh, A. Sohn, A.L. Weinstein, W.L. Olbricht, J. A. Spector, A portable high-intensity focused ultrasound device for noninvasive venous ablation, J. Vasc. Surg. 51 (2010) 707–711.
[11] C.J. Shaw, J. Civale, K.J. Botting, Y. Niu, G. ter Haar, I. Rivens, D.A. Giussani, C.C. Lees, Noninvasive high-intensity focused ultrasound treatment of twin-twin transfusion syndrome: a preliminary in vivo study, Sci. Transl. Med. 8 (347) (2016) 347ra95.
[12] S. Vaezy, R. Martin, P. Kaczkowski, G. Keilman, B. Goldman, H. Yaziji, S. Carter, M. Caps, L. Crum, Use of high-intensity focused ultrasound to control bleeding, J. Vasc. Surg. 29 (1999) 533–542.
[13] S. Vaezy, R. Martin, L. Crum, High intensity focused ultrasound: a method of hemostasis, Echocardiography 18 (2001) 309–315.
[14] S. Vaezy, R.W. Martin, U. Schmiedl, M. Caps, S. Taylor, K. Beach, S. Carter, P. Kaczkowski, G. Keilman, S. Helton, W. Chandler, P. Mourad, M. Rice, R. Roy, L. Crum, Liver hemostasis using high-intensity focused ultrasound, Ultrasound Med. Biol. 23 (1997) 1413–1420.
[15] S. Vaezy, R. Martin, H. Yazij, P. Kaczkowski, G. Keilman, S. Carter, M. Caps, E.Y. Chi, M. Bailey, L. Crum, Hemostasis of punctured blood vessels using high-intensity focused ultrasound, Ultrasound Med Biol. 24 (1998) 903–910.
[16] J.L. Teja, S.A. Lopez-Haro, L. Leija, A. Vera, A finite element simulation of high intensity focused ultrasound with polyacrylamide as coupling material for acoustic hemostasis, in: Proceedings of 2013 Pan American Health Care Exchanges (PAHCE).
[17] X. Zeng, S. Mitchell, M. Miller, S. Barnes, J. Hopple, J. Kook, R. Moreau-Gobard, S. Hsu, A. Ahiekpor-Dravi, L.A. Crum, J. Eaton, K. Wong, K.M. Sekins, Acoustic hemostasis of porcine superficial femoral artery: simulation and in-vivo experimental studies, AIP Conf. Proc. 1481 (2012) 475–480.
[18] M.A. Solovchuk, T.W.H. Sheu, M. Thiriet, Simulation of nonlinear Westervelt equation for the investigation of acoustic streaming and nonlinear propagation effects, J. Acoust. Soc. Am. 134 (2013) 3931–3942.
[19] M.A. Solovchuk, T.W.H. Sheu, M. Thiriet, Multiphysics modeling of liver tumor ablation by high intensity focused ultrasound, Commun. Comput. Phys. 18 (2015) 1050–1071.
[20] H.H. Pennes, Analysys of tissue and arterial blood temperature in the resting human forearm, J. Appl. Physiol. 1 (1948) 93–122.
[21] M.A. Solovchuk, T.W.H. Sheu, M. Thiriet, W.L. Lin, On a computational study for investigating acoustic streaming and heating during focused ultrasound ablation of liver tumor, J. Appl. Therm. Eng. 56 (2013) 62–76.
[22] M.A. Solovchuk, T.W.H. Sheu, M. Thiriet, Image-based computational model for focused ultrasound ablation of liver tumor, J. Comput. Surg. 1 (2014) 4.
[23] S. Vaezy, M.L. Noble, A. Keshavarzi, M. Paun, A.F. Prokop, C. Cornejo, S. Sharar, E.Y. Chi, L.A. Crum, R.W. Martin, Liver hemostasis with high-intensity ultrasound: repair and healing, J. Ultrasound Med. 23 (2004) 217–225.
[24] M.F. Hamilton, D.T. Blackstock, Nonlinear Acoustics, Academic Press, Boston, 1998.
[25] F.A. Duck, Physical Property of Tissues - A Comprehensive Reference Book, Academic, London, 1990.
[26] A. Sarvazyan, Diversity of biomedical applications of acoustic radiation force, Ultrasonics 50 (2) (2010) 230–234.
[27] A. Dayton, S. Zhao, S.H. Bloch, P. Schumann, K. Penrose, T.O. Matsunaga, R. Zutshi, Application of ultrasound to selectively localize nanodroplets for targeted imaging and therapy, Mol. Imag. 5 (3) (2006) 160–174.
[28] A.P. Sarvazyan, O.V. Rudenko, W.L. Nyborg, Biomedical applications of radiation force of ultrasound: historical roots and physical basis, Ultrasound Med. Biol. 36 (9) (2010) 1379–1394.
[29] R.W. Martin, S. Vaezy, P. Kaczkowski, G. Keilman, S. Carter, M. Caps, K. Beach, M. Plett, L. Crum, Hemostasis of punctured vessels using Doppler-guided high-intensity ultrasound, Ultrasound Med. Biol. 25 (1999) 985–990.
[30] J.W.S. Rayleigh, On the circulation of air observed in Kundt's tubes, and on some allied acoustical problems, Philos. Trans. R. Soc. Lond. 175 (1884) 1–21.
[31] C. Eckart, Vortices and streams caused by sound waves, Phys. Rev. 73 (1948), 676–76.
[32] W.L. Nyborg, Acoustic streaming due to attenuated plane waves, J. Acoust. Soc. Am. 25 (1953) 68–75.
[33] S. Tjotta, On some nonlinear effects in sound fields with special emphasis on the generation of vorticity and the formation of streaming patterns, Arch. Math. Naturvidensk 55 (1959) 1–68.
[34] T.W.H. Sheu, M.A. Solovchuk, A.W.J. Chen, M. Thiriet, On an acoustics-thermal-fluid coupling model for the prediction of temperature elevation in liver tumor, Int. J. Heat Mass Transfer 54 (17–18) (2011) 4117–4126.
[35] M.A. Solovchuk, T.W.H. Sheu, W.L. Lin, I. Kuo, M. Thiriet, Simulation study on acoustic streaming and convective cooling in blood vessels during a high-intensity focused ultrasound thermal ablation, Int. J. Heat Mass Transfer 55 (2012) 1261–1270.
[36] T. Kamakura, M. Matsuda, Y. Kumamoto, M.A. Breazeale, Acoustic streaming induced in focused Gaussian beams, J. Acoust. Soc. Am. 97 (1995) 2740–2746.
[37] M. Thiriet, Anatomy and Physiology of the Circulatory and Ventilatory Systems, Springer, New York, 2013.
[38] G.R. ter Haar, M. Dyson, S.P. Smith, Ultrastructural changes in the mouse uterus brought about by ultrasonic irradiation at therapeutic intensities in standing wave fields, Ultrasound Med. Biol. 5 (1979) 167–179.
[39] G.R. ter Haar, Ultrasonic biophysics, in: C.R. Hill, J.C. Bamber, G.R. ter Haar (Eds.), Physical Principles of Medical Ultrasonics, John Wiley and Sons, Chichester, 2004, pp. 349–407 (chap. 12).
[40] H.T. O'Neil, Theory of focusing radiators, J. Acoust. Soc. Am. 21 (1949) 516–526.
[41] D.T. Blackstock, Connection between the Fay and Fubini solutions for plane sound waves of finite amplitude, J. Acoust. Soc. Am. 14 (1966) 1019–1026.
[42] J. Huang, R.G. Holt, R.O. Cleveland, R.A. Roy, Experimental validation of a tractable medical model for focused ultrasound heating in flow-through tissue phantoms, J. Acoust. Soc. Am. 116 (2004) 2451–2458.
[43] M.A. Solovchuk, S.C. Hwang, H. Chang, M. Thiriet, T.W.H. Sheu, Temperature elevation by HIFU in ex-vivo porcine muscle: MRI measurement and simulation study, Med. Phys. 41 (2014) 052903, http://dx.doi.org/10.1118/1.4870965.
[44] J.W. Hand, Ultrasound hyperthermia and the prediction of heating, in: F.A. Duck, A.C. Baker, H.C. Starritt (Eds.), Ultrasound in Medicine, Institute of Physics Publishing, Bristol, 1998 (Ch. 8).
[45] S. Harnof, Z. Zibly, A. Hananel, S. Monteith, J. Grinfeld, G. Schiff, I. Kulbatski, N. Kassell, Potential of magnetic resonance-guided focused ultrasound for intracranial hemorrhage: an in vivo feasibility study, J. Stroke Cerebrovasc. Dis. 23 (6) (2014) 1585–1591.
[46] C.J. Shaw, G.R. ter Haar, I.H. Rivens, D.A. Giussani, C.C. Lees, Pathophysiological mechanisms of high-intensity focused ultrasound-mediated vascular occlusion and relevance to non-invasive fetal surgery, J. R. Soc. Interf. 11 (95) (2014) 20140029.
[47] R. Greaby, V. Zderic, S. Vaezy, Pulsatile flow phantom for ultrasound image-guided HIFU treatment of vascular injuries, Ultrasound Med. Biol. 33 (8) (2007) 1269–1276.